Monovalent maleimide functionalization of gold nanoparticles via copper-free click chemistry: A route to covalent nanoparticle-biomolecule conjugates

D. J. Nieves,[a] N.S. Azmi[a,b], R. Xu[a,c], R. Lévy[a], E. A. Yates[a] and D. G. Fernig[a,*]

[a] Institute of Integrative Biology, University of Liverpool, Crown Street, Liverpool, UK L69 7ZB. *E-mail: dgfernig@liv.ac.uk.
[b] Faculty of Industrial Sciences and Technology, Universiti Malaysia Pahang, Kuantan, Malaysia.
[c] Centre for Molecular Oncology, Barts Cancer Institute, Queen Mary, University of London, London, EC1M 6BQ.

Electronic Supplementary Information

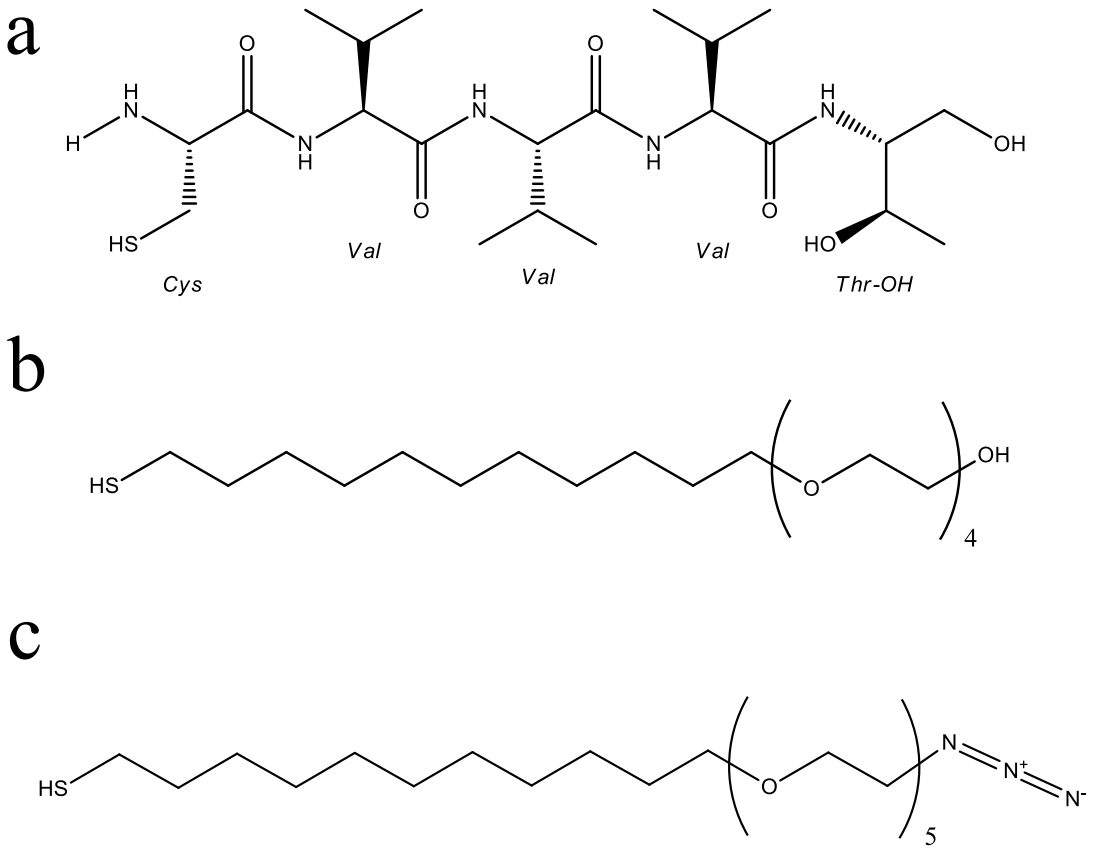

Fig. S1 Skeletal structures of thiol bearing ligands used for capping reaction to generate gold nanoparticle monolayer with azide functionality. a) CVVVT-ol peptidol, b) alkane thiol polyethylene glycol ($HS\text{-}C_{11}\text{-}(EG)_4\text{-}OH$) and c) alkane thiol polyethylene glycol bearing an azide group at the terminus ($HS\text{-}C_{11}\text{-}(EG)_5\text{-}N_3$).

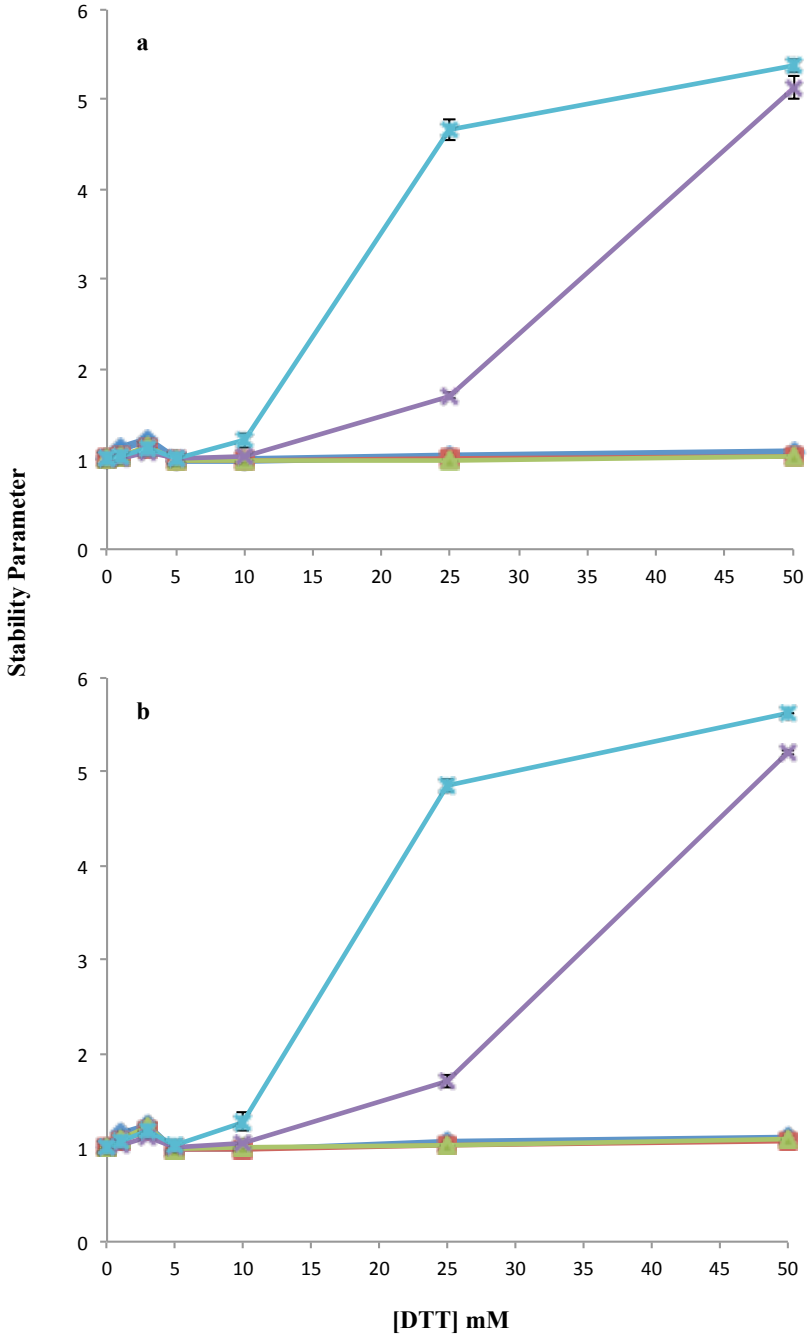

Fig. S2 Calculated stability parameter for a) mix-matrix and b) 1 % N_3 NPs in the presence of DTT. The stability parameter was taken at time points of 1 h (◆), 3 h (■), 6 h (▲), 24 h (×) and 48 h (✳). The stability parameter was measured and calculated exactly as described by Chen *et al.*[1], i.e., the absorbance at 650 nm (minus the reference of ddH_20) divided by the absorbance at 520 nm (again minus the reference of ddH_20). The calculated values were then normalised to the stability parameter calculated for capped nanoparticles in the absence of DTT at each time point. Here the stability parameter demonstrates that there is no significant exchange of ligands on the nanoparticles for DTT occurring up to 3 h at all concentrations and up to 10 mM over 24 h and 48 h.

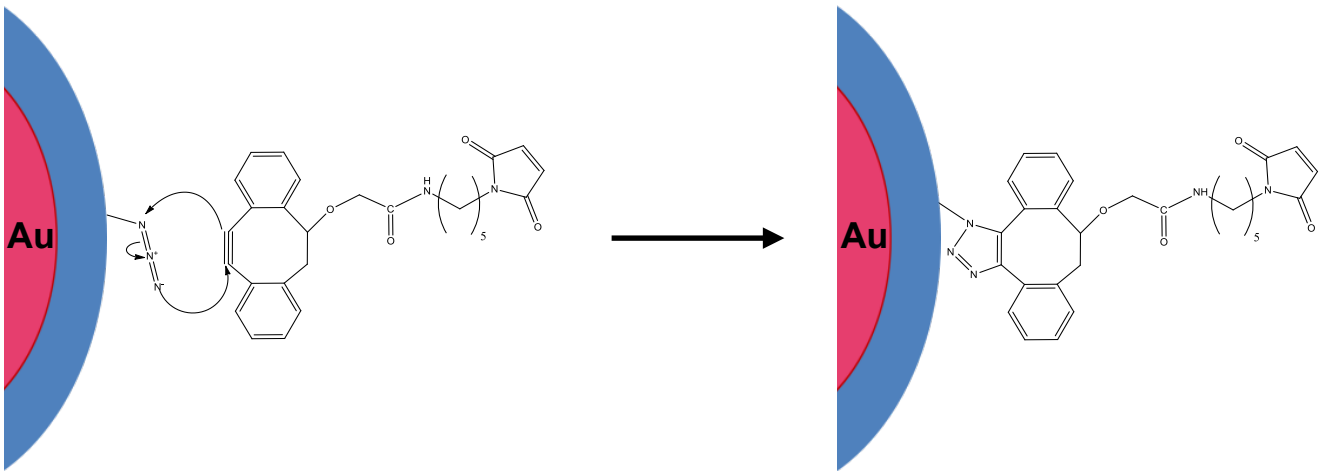

Fig. S3 Reaction scheme for DIBO-Mal with azide functionalised gold nanoparticles. The DIBO-Mal simultaneously acts as both a nucleophile and electrophile, attacking the azide functional group in the nanoparticle monolayer. This leads to the pericyclic formation of a triazole, thus installing maleimide functionality to the monolayer (blue).

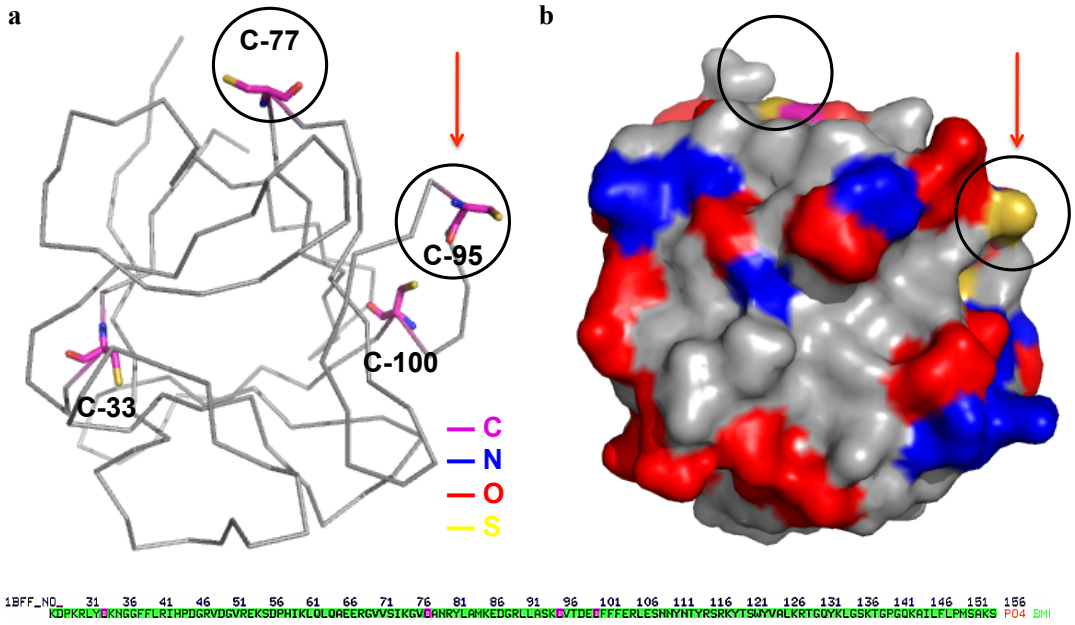

Fig. S4 Schematic of predicted three-dimensional structure of FGF-2 derived from PBD 1BFF [2] using PyMol. The structure of FGF-2 is represented in both ribbon (a) and electrostatic surface (b) forms. The cysteines present within FGF-2 are denoted in the amino acid sequence (pink, bottom). All cysteines in FGF-2 are denoted in (a), whereas only the cysteines with solvent exposed thiol side chains are visible in (b) and ringed in both structures (black). The most exposed cysteine, C-95, and a candidate for Michael addition to the nanoparticle is marked with the arrow (red).

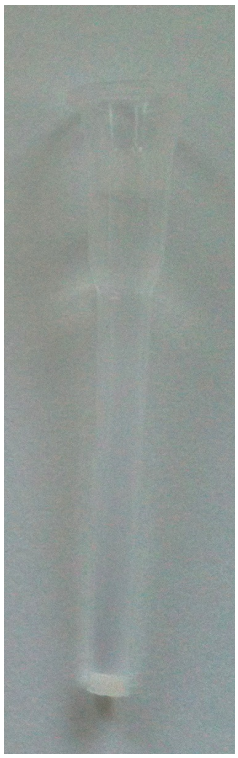

Fig. S5 Heparin affinity chromatography of Mal-NPs mixed with blocked FGF2 protein. The surface thiols of FGF2 were reacted with a molar excess of biotin-maleimide (N-Biotinoyl-N'-(6-maleimidohexanoyl)hydrazide; Sigma Aldrich) prior to incubation with Mal-NPs. Removal of excess biotin-maleimide was achieved by heparin affinity chromatography of FGF2 and washing with 3 column volumes of $PBST_{0.05\%}$. Blocked FGF2 was then eluted from the column with 2 M NaCl. Te blocked FGF2 was then incubated in a molar excess over Mal-NPs for 3 h with mixing on a wheel. The mixture was then passed through a heparin affinity column, and washed with 3 column volumes of $PBST_{0.05\%}$. No Mal-NPs bound the column indicating that the thiol-Michael addition reaction with FGF2 was prevented due to the prior blocking step.

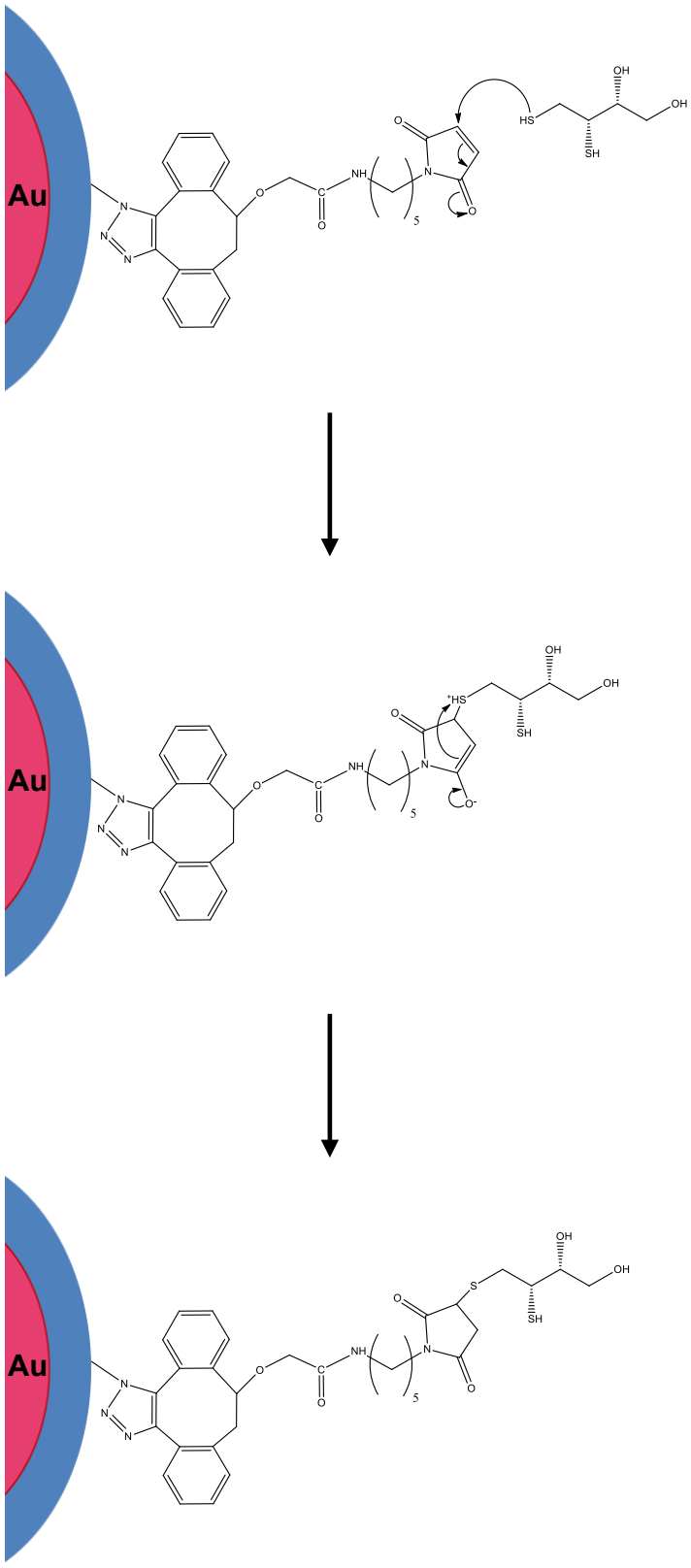

Fig. S6 Exemplar reaction scheme for thiol-Michael addition reaction between maleimide functionalised gold nanoparticles and dithiothreitol (DTT). The double bond of the maleimide is attacked by a nucleophillic thiol group of DTT. This leads to the formation of a stable thioether bond, which in the case of DTT yields a free, external of the monolayer (blue), thiol group for further thiol-Michael reactions

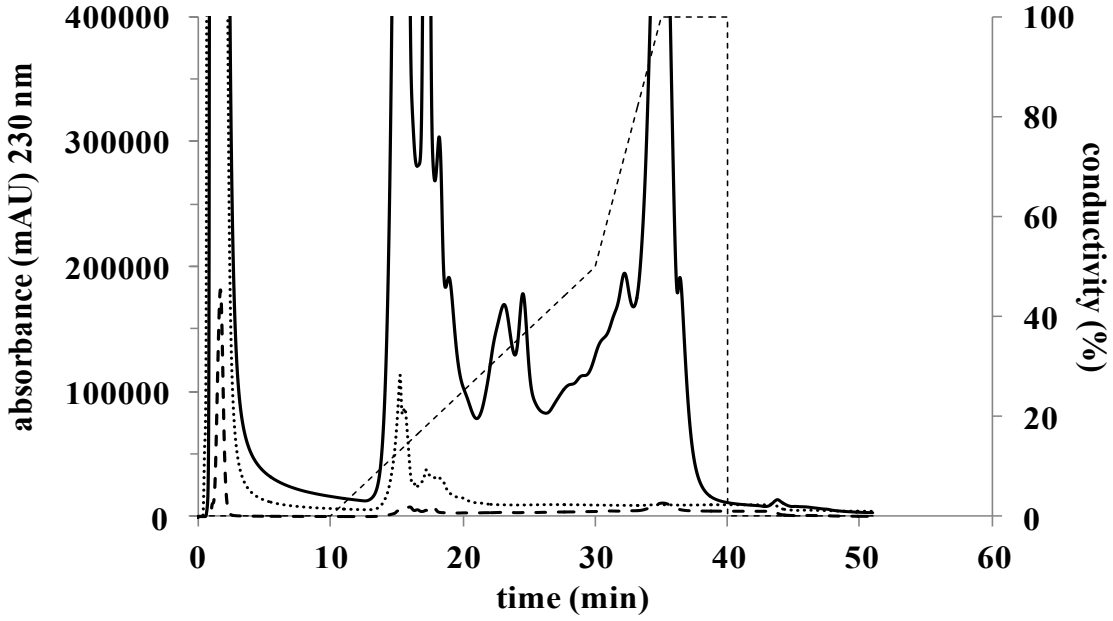

Fig. S7 Anion-exchange chromatography of the products from the reaction of MPBH (4-(4-N-Maleimidophenyl)butyric acid hydrazide-HCl; Thermo Fischer Scientific Inc., Rockford, IL, USA) and heparin-derived oligosaccharide degree of polymerisation (dp) 12 in formamide. Analysis of the products of the reaction of MPBH (15 mg/mL) and dp12 (1 mg) in formamide using anion-exchange chromatography (230 nm) using a HiTrap Q column (1 mL) equilibrated with HPLC grade water (Fisher Scientific, Loughborough, UK). After loading the sample, the column was developed with a gradient of 2 M NaCl in the same buffer at a flow rate of 1 mL/min (----). The dp12 control (----): 100 µL of 1 mg freeze-dried dp12 in HPLC grade water. MPBH control (••••): 100 µL of 15 mg/mL MPBH dissolved in formamide with 2.5 µL of acetic acid and 400 µL of HPLC grade water. MPBH and dp12 reaction product (—): dissolved in 400 µL HPLC grade water.

Table S1 Compound purity of porcine intestinal mucosal heparin.

The starting material for all chemical modifications was porcine intestinal mucosal heparin (CelsusLabs, Cincinnati, OH, USA; lot PH-42800 with anticoagulant activity 201 IU.mg-1).

The polysaccharide was subjected to purification by size-exclusion chromatography (Sephadex G-25, recovering only the exclusion limit; Mw> 5 KDa) and treated with ion exchange resin (Dowex, W-50, Na^+ form) prior to NMR and activity testing.

Size-exclusion chromatography analysis of the polysaccharide was also conducted with a TSK gel G2000SWXL column (7.8 mm x 30 cm with 0.5 μm particle size; Supelco) eluting with water at 1 mL/min and detecting at 190 nm. All the samples exhibited a single major peak (>95 %), with very similar retention times (mean, 6.07 minutes; Dn-1=0.05).

Porcine mucosal heparin was also exhaustively digested with a mixture of heparitinases I, II and III to their constituent disaccharides (here denoted 1 to 8). Disaccharides were separated by strong-anion exchange HPLC (Propac PA-1 column, Dionex UK) and quantified (A232) with reference to authentic standards (Dextra Labs, Reading, UK) and showed the following composition (%). In all cases, unidentified peaks were < 5% of the total area of the constituents[3].

	Disaccharide ✣							
Porcine Mucosal Heparin	1	2	3	4	5	6	7	8
	6.8	-	3.4	13.4	7.0	67.4	-	8.0

✣ Standards: 1, ΔUA-GlcNAc; 2, ΔUA-GlcNAc(6S); 3, ΔUA-GlcNS; 4, ΔUA-GlcNS(6S); 5, ΔUA(2S)-GlcNS; 6, ΔUA(2S)-GlcNS(6S); 7, ΔUA(2S)-GlcNAc and 8, ΔUA(2S)-GlcNAc(6S), where GlcNAc is N-acetyl glucosamine, ΔUA is the uronic acid (glucuronate or iduronate, which cannot be distinguished), 6S and 2S refer to ester O-sulfates on the respective carbon of the sugar, NS to the amino sugar on C2 of the glucosamine.

Table S2 ^{1}H and ^{13}C NMR chemical shift values for porcine intestinal mucosal heparin.

The porcine mucosal heparin was characterized by ^{1}H and ^{13}C NMR to confirm its structure. NMR spectra were recorded in D_2O at 40 °C on a 400 MHz instrument. Assignment was by a combination of COSY, TOCSY, HMBC two-dimensional spectra. ^{13}C spectra were recorded on 150 mg samples of the heparin. Chemical shift values were recorded relative to trimethylsilyl propionate as reference standard at 40 °C[3].

	Glucosamine						Iduronate				
	A-1	A-2	A-3	A-4	A-5	A-6	I-1	I-2	I-3	I-4	I-5
Porcine	99.5	60.7	72.5	78.8	72.0	69.2	102.1	78.9	72.1	79.0	72.3
Mucosal Heparin	5.42	3.31	3.69	3.79	4.05	4.30-4.42	5.23	4.37	4.22	4.14	4.82

References

1. X. Y. Chen, W. W. Qoutah, P. Free, J. Hobley, D. G. Fernig and D. Paramelle, *Aust J Chem*, 2012, 65, 266-274.
2. J. S. Kastrup, E. S. Eriksson, H. Dalboge and H. Flodgaard, *Acta Crystallogr Sect D-Biol Crystallogr*, 1997, 53, 160-168.
3. M. A. Skidmore, A. F. Dumax-Vorzet, S. E. Guimond, T. R. Rudd, E. A. Edwards, J. E. Turnbull, A. G. Craig and E. A. Yates, *J Med Chem*, 2008, 51, 1453-1458.